



Robustness and accuracy of model-free structural health monitoring

M. Rabiepour, C. Zhou, J.G. Chase & G.W. Rodgers

University of Canterbury, Department of Mechanical Engineering, Christchurch.

C. Xu

Northwestern Polytechnical University, Department of Astronautics, Xi'an, China.

ABSTRACT

Rapid, accurate structural health monitoring (SHM) assesses damage to optimise decision-making. Many SHM methods are designed to track nonlinear stiffness changes as damage. However, highly nonlinear pinched hysteretic systems are problematic in SHM. Model-based SHM often fails as any mismatch between model and measured response dynamics leads to significant error. Thus, model-free methods of hysteresis loop tracking methods have emerged. This study compares the robustness and accuracy in the presence of significant measurement noise of the proven hysteresis loop analysis (HLA) SHM method with 3 emerging model-free methods and 2 further novel adaptations of these methods using a highly nonlinear, 6-story numerical structure to provide a known ground-truth.

Mean absolute errors in identifying a known nonlinear stiffness trajectory assessed at four points over two successive ground motion inputs from September 2010 and February 2011 in Christchurch range from 1.71-10.52%. However, the variability is far wider with maximum errors ranging from 3.90-49.72%, where the second largest maximum absolute error was still 19.74%. The lowest mean and maximum absolute errors were for the HLA method. The next best method had mean absolute error of 2.92% and a maximum of 10.51%.

These results show the clear superiority of the HLA method over all current emerging model-free methods designed to manage the highly nonlinear pinching responses common in reinforced concrete structures. These results, combined with high robustness and accuracy in scaled and full-scale experimental studies, provide further validation for using HLA for practical implementation.

1 INTRODUCTION

It is important to assess damage after an earthquake. The lack of reliable, accurate SHM methods led to significant disagreements about the level of damage and remaining lifetime of structures in Christchurch, New Zealand after the events of 2010-2011, delaying repair and recovery (Clifton 2011, Johnson 2016).

The primary purpose of SHM methods is detecting the presence, location, and the severity of damage after major external loads (Doebbling 1998, Housner 1997). Existing structural damage identification methods typically fall into model-based and model-free methods (Fan 2011). In model-based methods, a computer model of the real structure is identified by comparing model simulated and measured responses e.g. (Chase 2005a, 2005b, 2005c, Nayyerloo 2011, Zhou 2017d). Model-free methods depend only on the measured responses by sensors e.g. (Xu 2014, Zhou 2016, 2017a, 2019, 2017b, 2015, 2017d).

Model-based methods can successfully assess damage when the adopted baseline model contains the observed dynamics of the real structure. However, there is always some uncertainty in selecting a baseline model and its dynamics, particularly for nonlinear cases. Any mismatch increases the risk of incorrect damage estimation for model-based methods, limiting their ability (Zhou 2017d). In addition, most model-based and many model-free methods require human input to guide identification, limiting applicability after an event (Zhou 2016).

Lately, a multiple linear regression approach has accurately identified linear and nonlinear structural stiffness from force-deformation loops across multiple events with inter-event consistency not displayed by other methods, which often does not even consider this consistency between events (Xu 2015, 2014, Zhou 2017a, 2015). This hysteresis loop analysis (HLA) method is fully automated, unlike many SHM methods, and has been validated on full-scale and test structures (Zhou 2017a, 2019, 2017b, 2017d).

This study compares the capability of HLA with some Piecewise Linear Representation (PLR) based SHM methods (Keogh 2001, Salvador 2004) to identify the evolution of elastic stiffness for a numerical 6-story structure with highly nonlinear hysteretic pinched behaviour under two successive earthquakes of September 2010 and February 2011 hit Christchurch.

2 SHM METHODS

2.1 Numerical model

Mechanical properties of the 6-story numerical structure is summarised in Table 1, and the highly nonlinear pinching behaviour simulated by a slip-lock Baber-Noori model (Baber 1985, 1986) is depicted schematically in Figure 1. The dynamic equation of motion for the building under a seismic vibration is:

$$F(t) = -MI\ddot{x}_g(t) - M\ddot{X}(t) - C\dot{X}(t) \quad (1)$$

where M and C are the mass and damping matrices, \dot{X} and \ddot{X} are vectors of structural velocity and acceleration, and \ddot{x}_g is the input seismic acceleration. $F(t)$ is the nonlinear restoring force vector, which is decoupled to the inter-story restoring force, $f(t)$, for each floor, i :

$$f_i(t) = \sum_{j=i}^{nstory} F_j(t) \quad (2)$$

where $nstory$ is the number of stories, and $f(t)$ is defined (Baber 1985, 1986, Wen 1976) :

$$f(t) = \alpha K_0 x + (1 - \alpha) K_0 z \quad (3)$$

where K_0 and α are the initial elastic stiffness and post-yielding ratio, respectively. The relationship between the inter-story-displacement, x , and hysteretic displacement, z , can be obtained for each story (Baber 1985, 1986, Pellicciari 2018, Sengupta 2013):

Story	Mass (Kg)	Initial stiffness (kN/m)
1	200	450
2	250	350
3	250	300
4	275	400
5	285	500
6	285	600

5% Damping ratio for the first two modes.

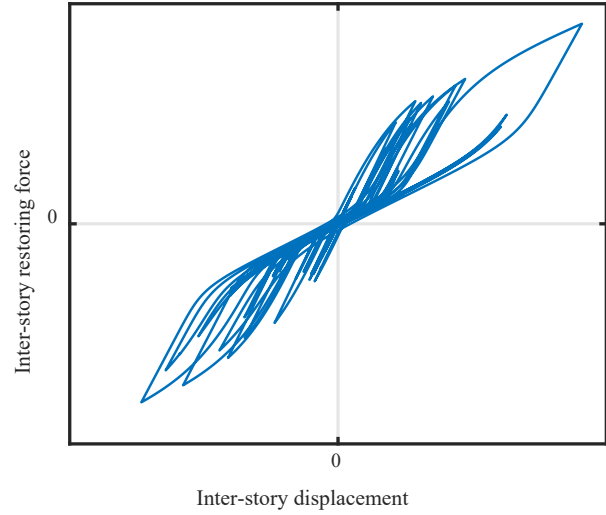


Table 1: Mechanical properties of the numerical 6-story structure.

Figure 1: Schematic image depicting highly nonlinear pinching behavior.

$$\frac{\dot{z}}{\dot{x}} = h(z) \times \frac{A - v(\beta \text{sign}(\dot{x}z) + \gamma)|z|^n}{\eta} \quad (4)$$

where A , β , n and γ are the dimensionless shape parameters of hysteretic loops, sign is the signum function. The parameters η and v are the stiffness and strength degradation functions defined:

$$\eta(t) = 1 + \delta_\eta \varepsilon(t) \quad (5)$$

$$v(t) = 1 + \delta_v \varepsilon(t) \quad (6)$$

$$\varepsilon(t) = (1 - \alpha) \frac{K_e}{m} \int_0^t z(\tau) \dot{x}(\tau) d\tau \quad (7)$$

where $\varepsilon(t)$ is the total dissipated energy, and the constants δ_η and δ_v determine the rate of strength and stiffness degradation. The term $h(z)$ in Equation 4 is the pinching function:

$$h(z) = 1 - \xi_1 e^{-\left(\frac{z \text{sign}(\dot{x}) - qz_u}{\xi_2}\right)^2} \quad (8)$$

where the pinching initiation parameter, q , is a constant and the ultimate value of z , given by z_u , is defined:

$$z_u(t) = n \sqrt{\frac{1}{v(\beta + \gamma)}} \quad (9)$$

$$\xi_1(t) = \xi_0 (1 - e^{-p\varepsilon(t)}) \quad (10)$$

$$\xi_2(t) = (\psi + \delta_\psi \varepsilon) \times (\lambda + \xi_1) \quad (11)$$

where ξ_0 is the measure of total slip, p controls the pinching slope, ψ is a constant contributing to the pinching magnitude, δ_ψ is a constant controlling the pinching rate, and λ is a small constant controlling the variation of parameters ξ_1 and ξ_2 (Pellicciari 2018). The required parameters for the Bouc-Wen-Baber-Noori (BWBN) model are summarised in Table 2.

The structure is subjected to two successive earthquakes and estimated elastic stiffness is compared with the true values at four specific stages as shown in Figure 2. Stages I and III assess initial estimates at the

beginning of two major events. Stages II and III assess accuracy across events. Finally, Stages II and IV assess accuracy over a single major event.

Table 2: BWBN model parameters for the numerical structure.

Story	α	p	q	λ	ψ	ξ_0	δ_ψ	δ_η	δ_ν
1 - 5	0.2	0.2	0.01	0.05	0.1	0.95	0.001	0.001	0.001
6	0.2	0.2	0.01	0.01	0.1	0.95	0.005	0.001	0.001

with the shape parameters of $A = 1$, $\beta = 0.5$, $\gamma = 0.5$, $\nu = 1$ and $n = 2$.

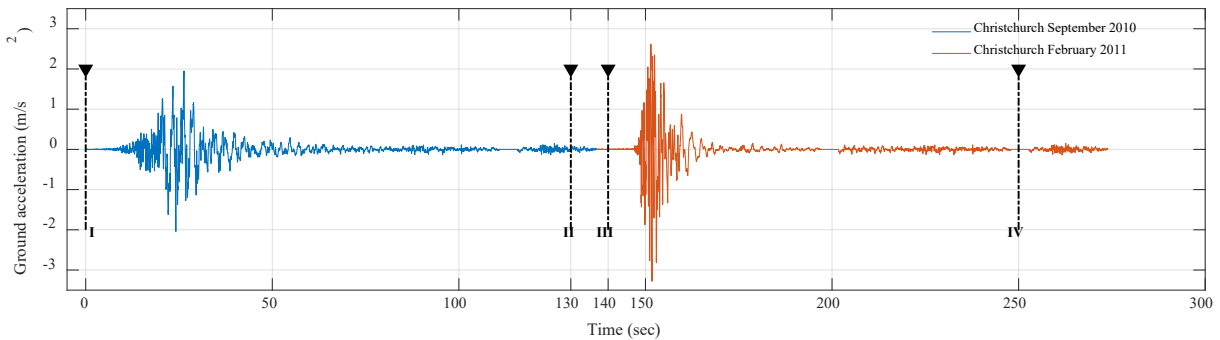


Figure 2: Four stages (I-IV) to compare estimated elastic stiffness of the numerical building over the Christchurch earthquakes of September 2010 and February 2011.

2.2 HLA method

The model-free, mechanics-relevant HLA method, as given in detail in (Zhou 2017b, 2015), uses regression and a hypothesis test to estimate elastic stiffness evolution from reconstructed hysteresis loops. HLA is computationally straightforward and automated, with no user-input required. It performs in real-time for each half cycle. Therefore, SHM results can be available after an earthquake (Zhou 2017a, 2017b, 2017c, 2015).

2.3 PLR-based methods

PLR-based techniques are model-free methods, where a half cycle of length N , is approximated by K linear segments whose slopes represent stiffness. Most PLR-based algorithms can be classified into one of the three main groups: 1- Sliding Windows (SW), 2- Top-Down (TD), and 3- Bottom-Up (BU). These algorithms are introduced in details and their pseudocodes are available in (Keogh 2001, Salvador 2004).

The regression process in these methods terminates until a stopping criteria is met. Here, the regression standard error with a threshold of $SE=10$ chosen to play this role. Thus, results of these methods can be very sensitive to thresholds, and cannot be easily automated. Moreover, models created by these algorithms are typically disjointed with non-continuous derivatives. To address these issues, modified versions of SW and TD methods: 4- Constrained Sliding Windows (CSW), and 5- Modified Top-Down (MTD) are proposed.

CSW is proposed to produce a smoother model. In CSW, the first point of the first linear segment is $(0,0)$, from which the slope of the best line fit to the data points creates the first linear segment. For the second segment, the line is constrained to cross the last point of the previous fitted segment. This process repeats for the next segments until the half-cycle reconstruction is complete.

The MTD method is proposed to decrease the sensitivity of PLR-based methods to the user-specified threshold and the presence of noise. In the MTD method, each half-cycle is checked to see if it can be represented just by a single linear segment or not. If the R-squared R^2 value of this linear segment is above a user-selected minimum value, it can be modelled by one segment. Otherwise, the half-cycle must be further divided. In this study, the R-squared threshold is $R^2 = 0.99$ for noise-free conditions and $R^2 = 0.95$ for noisy cases. These values usually remain unchanged and avoid overfitting.

Since structural hysteresis loops have a range of known fundamental patterns, the maximum number of breakpoints can be estimated as $(7 = 2^3 - 1)$ for half-cycles with pinched nonlinear behavior. The best locations of these breakpoints are obtained by the recursive approach employed in the TD algorithm. Extra breakpoints must be pruned to prevent overfitting. For pruning, small segments are merged with adjacent segments. In this paper, the minimum length of the segments is limited to 3 samples.

2.4 Analyses

To compare the performance of the SHM methods, 10% root mean square (RMS) noise is added to simulated measurements sampled at 250Hz rate (Zhou 2016). Because of the random nature of noise, each method is run 20 times and the average results are reported in a Monte Carlo approach similar to (Moghaddasi 2011).

3 RESULTS AND DISCUSSION

Table 3 compare methods with 10% added RMS noise and without noise at a realistic sampling rate of 250Hz. As expected, noise reduce the accuracy of all methods. Although, TD is the least robust method to noise with the maximum error of 49.72% , MTD works significantly better in noisy conditions. Maximum error of all methods, except HLA, is higher than 10% in the presence of noise, which makes them unreliable. The mean error of HLA only increased by 1.09% to 1.71% when 10% noise is added. Therefore, HLA is highly robust to sensor noise and considerably better than the other methods presented here.

Table 3: Maximum and mean absolute errors for elastic stiffness over all 6 stories for each SHM method (Noise = 0% ,10% ; Sampling rate = 250Hz); Results are reported in percent.

	Noise-free			10% Noise		
	Mean	Max	SD	Mean	Max	SD
SW	0.76	5.40	1.13	4.80	13.29	4.00
CSW	0.57	4.51	0.93	2.99	13.76	3.28
BU	0.34	1.03	0.29	4.75	19.74	4.46
TD	0.40	1.07	0.35	10.52	49.72	13.63
MTD	0.31	1.30	0.34	2.92	10.51	2.54
HLA	0.62	1.85	0.37	1.71	3.90	1.10

Figure 3 compares the performance of HLA with the other methods in identifying the evolution of elastic stiffness for the 6th floor in the noisy condition. It is visually apparent the estimated elastic stiffness at stages II and III are almost equal for all methods, which is essential for a reliable SHM method. All the methods, except SW, worked slightly better than HLA in identifying the initial stiffness at Stage I, but not enough to guarantee better accuracy or to be meaningful in decision-making, as Stage I is the before event value. At the other stages, HLA significantly performs better.

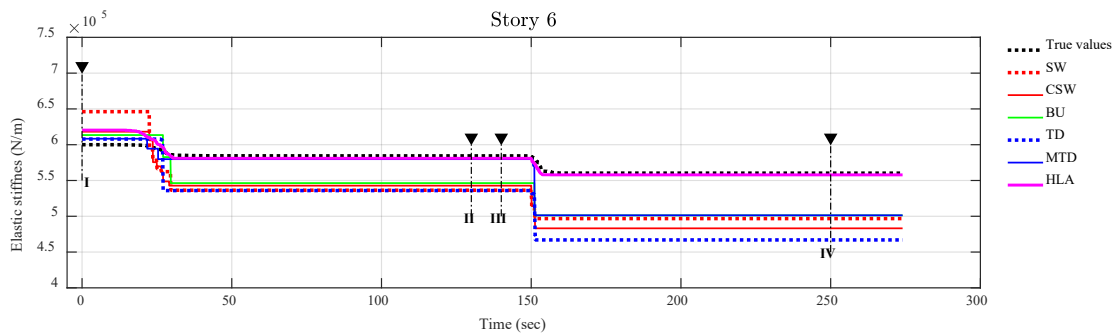


Figure 3: Elastic stiffness of Story 6 estimated by the SHM methods (Noise = 10%; Sampling rate = 250Hz) .

PLR-based algorithms require always some human-input parameters to be tuned (Keogh 2001, Salvador 2004). So they are not general or automated. Moreover, their accuracy is too sensitive to the level of sensor noise, as seen in the results. Although the modifications applied made MTD more robust to noise compared to the other PLR-based algorithms, it was not sufficient to challenge the HLA. Moreover, MTD still depends on human inputs and render the algorithm less general.

HLA requires no human inputs and determines the evolution of elastic stiffness over time from the measured responses automatically. Results show HLA, as expected, is very robust to sensor noise. HLA performance for noisy and real-world conditions has been proven numerically and experimentally (Zhou 2016, 2017a, 2019, 2017b, 2017c, 2017d).

A single test structure with a full range of nonlinearity should be employed to test the robustness of the methods and validate these simulated-based results over all methods. HLA is already well-proven for full-scale and scaled test structures on several studies (Zhou 2017a, 2019, 2017b, 2017c, 2017d).

4 CONCLUSIONS

In this paper, five model-free methods are employed to challenge HLA for identifying structural elastic stiffness. For this purpose, a simulated highly nonlinear pinched hysteretic structure is subjected to two major earthquakes to investigate their robustness, consistency and accuracy. Identified stiffness values are compared to simulated known values at four Stages (I-IV) across two events for each method.

- HLA is the most accurate method, particularly when avoiding maximum errors.
- The overall results show how methods can vary significantly despite similarities.
- HLA is implemented in an automated function requiring no user input, while all model-free PLR-based methods need human inputs and priori knowledge to be tuned for a good performance.

REFERENCES

- Baber, T.T. & Noori, M.N. 1985. Random Vibration of Degrading, Pinching Systems. *Journal of Engineering Mechanics-Asce* 111 (8): 1010-1026.
- Baber, T.T. & Noori, M.N. 1986. Modeling General Hysteresis Behavior and Random Vibration Application. *Journal of Vibration Acoustics Stress and Reliability in Design-Transactions of the Asme* 108 (4): 411-420.
- Chase, J.G., Begoc, V. & Barroso, L.R. 2005a. Efficient structural health monitoring for a benchmark structure using adaptive RLS filters. *Computers & structures* 83 (8-9): 639-647.
- Chase, J.G., Hwang, K.L., Barroso, L.R. & Mander, J.B. 2005b. A simple LMS-based approach to the structural health monitoring benchmark problem. *Earthquake engineering & structural dynamics* 34 (6): 575-594.
- Chase, J.G., Spieth, H.A., Blome, C.F. & Mander, J. 2005c. LMS-based structural health monitoring of a non-linear rocking structure. *Earthquake engineering & structural dynamics* 34 (8): 909-930.

- Clifton, C., Bruneau, M., MacRae, G., Leon, R. & Fussell, A. 2011. Steel structures damage from the Christchurch earthquake series of 2010 and 2011. *Bulletin of the New Zealand Society for Earthquake Engineering* 44 (4): 297-318.
- Doebling, S.W., Farrar, C.R. & Prime, M.B. 1998. A summary review of vibration-based damage identification methods. *Shock and vibration digest* 30 (2): 91-105.
- Fan, W. & Qiao, P. 2011. Vibration-based damage identification methods: a review and comparative study. *Structural health monitoring* 10 (1): 83-111.
- Housner, G.W., Bergman, L.A., Caughey, T.K., Chassiakos, A.G., Claus, R.O., Masri, S.F., Skelton, R.E., Soong, T., Spencer, B. & Yao, J.T. 1997. Structural control: past, present, and future. *Journal of engineering mechanics* 123 (9): 897-971.
- Johnson, L.A. & Olshansky, R.B. 2016. *After great disasters: how six countries managed community recovery*. Lincoln Institute of Land Policy.
- Keogh, E., Chu, S., Hart, D. & Pazzani, M. 2001. An Online algorithm for segmenting time series. *2001 Ieee International Conference on Data Mining, Proceedings*.289-296.
- Moghaddasi, M., Cubrinovski, M., Chase, J.G., Pampanin, S. & Carr, A. 2011. Effects of soil-foundation-structure interaction on seismic structural response via robust Monte Carlo simulation. *Engineering Structures* 33 (4): 1338-1347.
- Nayyerloo, M., Chase, J., MacRae, G. & Chen, X. 2011. LMS-based approach to structural health monitoring of nonlinear hysteretic structures. *Structural Health Monitoring* 10 (4): 429-444.
- Pellicciari, M., Marano, G.C., Cuoghi, T., Briseghella, B., Lavorato, D. & Tarantino, A.M. 2018. Parameter identification of degrading and pinched hysteretic systems using a modified Bouc–Wen model. *Structure and Infrastructure Engineering* 14 (12): 1573-1585.
- Salvador, S. & Chan, P. 2004. Determining the number of clusters/segments in hierarchical clustering/segmentation algorithms. *Ictai 2004: 16th Ieee Internationalconference on Tools with Artificial Intelligence, Proceedings*.576-584.
- Sengupta, P. & Li, B. 2013. Modified Bouc–Wen model for hysteresis behavior of RC beam–column joints with limited transverse reinforcement. *Engineering Structures* 46 392-406.
- Wen, Y. 1976. Method for random vibration of hysteretic systems. *Journal of the engineering mechanics division* 102 (2): 249-263.
- Xu, C., Chase, J.G. & Rodgers, G.W. 2015. Nonlinear regression based health monitoring of hysteretic structures under seismic excitation. *Shock and Vibration* 2015
- Xu, C., Chase, J.G., Rodgers, G.W. & Zhou, C. 2014. Multi-Phase Linear Regression: A Novel Method for the Identification of Base-Isolated Buildings Using Seismic Response Data. *Eurodyn 2014: 1x International Conference on Structural Dynamics*.2599-2604.
- Zhou, C. 2016. Efficient hysteresis loop analysis based structural health monitoring of civil structures. PhD Thesis Mechanical Engineering, University of Canterbury, Christchurch, New Zealand.
- Zhou, C., Chase, J.G. & Rodgers, G. 2017a. Efficient hysteresis loop analysis-based damage identification of a reinforced concrete frame structure over multiple events. *Journal of Civil Structural Health Monitoring* 7 (4): 541-556.
- Zhou, C., Chase, J.G. & Rodgers, G.W. 2019. Degradation evaluation of lateral story stiffness using HLA-based deep learning networks. *Advanced Engineering Informatics* 39 259-268.
- Zhou, C., Chase, J.G., Rodgers, G.W., Huang, B.F. & Xu, C. 2017b. Effective Stiffness Identification for Structural Health Monitoring of Reinforced Concrete Building using Hysteresis Loop Analysis. *X International Conference on Structural Dynamics (Eurodyn 2017)* 199 1074-1079.
- Zhou, C., Chase, J.G., Rodgers, G.W. & Iihoshi, C. 2017c. Damage assessment by stiffness identification for a full-scale three-story steel moment resisting frame building subjected to a sequence of earthquake excitations. *Bulletin of Earthquake Engineering* 15 (12): 5393-5412.
- Zhou, C., Chase, J.G., Rodgers, G.W., Tomlinson, H. & Xu, C. 2015. Physical parameter identification of structural systems with hysteretic pinching. *Computer-Aided Civil and Infrastructure Engineering* 30 (4): 247-262.
- Zhou, C., Chase, J.G., Rodgers, G.W. & Xu, C. 2017d. Comparing model-based adaptive LMS filters and a model-free hysteresis loop analysis method for structural health monitoring. *Mechanical Systems and Signal Processing* 84 384-398.